Colloids and Surfaces B: Biointerfaces 132 (2015) 208–215

Contents lists available at ScienceDirect

Colloids and Surfaces B: Biointerfaces

journal homepage: www.elsevier.com/locate/colsurfb

45S5Bioglass®-based scaffolds coated with selenium nanoparticles or with poly(lactide-co-glycolide)/selenium particles: Processing, evaluation and antibacterial activity

Magdalena Stevanović[a,*], Nenad Filipović[a], Jelena Djurdjević[a], Miodrag Lukić[a], Marina Milenković[b], Aldo Boccaccini[c]

[a] Institute of Technical Sciences of the Serbian Academy of Sciences and Arts, 11000 Belgrade, Serbia
[b] Department of Microbiology and Immunology, Faculty of Pharmacy, University of Belgrade, 11000 Belgrade, Serbia
[c] Institute of Biomaterials, Department of Materials Science and Engineering, University of Erlangen-Nuremberg, 91058 Erlangen, Germany

ARTICLE INFO

Article history:
Received 6 January 2015
Received in revised form 27 March 2015
Accepted 13 May 2015
Available online 22 May 2015

Keywords:
Scaffold
Bioglass
Selenium nanoparticles
PLGA
Antibacterial activity

ABSTRACT

In the bone tissue engineering field, there is a growing interest in the application of bioactive glass scaffolds (45S5Bioglass®) due to their bone bonding ability, osteoconductivity and osteoinductivity. However, such scaffolds still lack some of the required functionalities to enable the successful formation of new bone, e.g. effective antibacterial properties. A large number of studies suggest that selenium (Se) has significant role in antioxidant protection, enhanced immune surveillance and modulation of cell proliferation. Selenium nanoparticles (SeNp) have also been reported to possess antibacterial as well as antiviral activities. In this investigation, uniform, stable, amorphous SeNp have been synthesized and additionally immobilized within spherical PLGA particles (PLGA/SeNp). These particles were used to coat bioactive glass-based scaffolds synthesized by the foam replica method. Samples were characterized by X-ray diffraction (XRD), Fourier transform infrared spectroscopy (FTIR), scanning electron microscopy (SEM), energy dispersive X-ray spectroscopy (EDS) and transmission electron microscopy (TEM). SeNp, 45S5Bioglass®/SeNp and 45S5Bioglass®/PLGA/SeNp showed a considerable antibacterial activity against Gram positive bacteria, *Staphylococcus aureus* and *Staphylococcus epidermidis*, one of the main causative agents of orthopedic infections. The functionalized Se-coated bioactive glass scaffolds represent a new family of bioactive, antibacterial scaffolds for bone tissue engineering applications.

1. Introduction

Bone tissue is the major structural and supportive connective tissue composed of about 25% water, 25% protein i.e. collagen fibers, and 50% mineral salts of which the most calcium and phosphorous salts. It is a dynamic, highly vascularized tissue with the major role to provide structural support for the body [1]. The worldwide incidence of bone disorders and conditions significantly increases recently and it is expected to double by 2020 [2]. The field of bone tissue engineering was initiated a few decades ago and is based on the understanding of bone structure, bone mechanics, and tissue formation [1,2]. Bone tissue engineering aims to successfully regenerate or repair bone and applies methods from materials engineering and life sciences to produce artificial or natural constructs [3,4]. There are several approaches for the regeneration or for the formation of the new tissue. One is to isolate specific cells from a patient and to grow them on a three-dimensional scaffold after which the construct will be delivered to the desired site in the patient's body aiming to direct new tissue formation into the scaffold [3]. Another way is to implant scaffold for tissue ingrowth directly in vivo to stimulate and to direct tissue formation in situ [3–5]. Biomaterials for scaffolds preparation have to possess certain physical, chemical, and biological properties [6–8]. However, it is difficult for any biomaterial to satisfy all of the requirements which led to the development of wide variety of composites or hybrid materials. These hybrid materials are made by combination of two or more biomaterials, with enhanced functionalities, in the form of polymer–polymer blends, organic–inorganic hybrids and polymer–ceramic composites [3,9–12]. Recently, there is a growing interest in the application of bioactive silicate glasses due to their bone bonding ability and osteoconductivity [13,14]. In addition,

* Corresponding author at: Institute of Technical Sciences of the Serbian Academy of Sciences and Arts, Knez Mihailova 35/IV, 11000 Belgrade, Serbia. Tel.: +381 11 2636 994; fax: +381 11 2185 263.
E-mail addresses: magdalena.stevanovic@itn.sanu.ac.rs, magir@eunet.rs (M. Stevanović).

http://dx.doi.org/10.1016/j.colsurfb.2015.05.024
0927-7765/

these highly surface reactive materials exhibit osteogenic and angiogenic effects [13]. Structural 3D bioactive glass scaffolds with suitable interpenetrating porosity and mechanical stability have been developed in recent years [14–16]. However such scaffolds still lack some of the required functionalities to enable the successful formation of new vascularized bone in critical size bone defects, e.g. enhanced bioactivity by incorporation of bioactive molecules or growth factors and effective antibacterial properties. Additionally, the angiogenic and antibacterial characteristics of scaffolds are now being examined in more detail, the goal being to integrate these functions in a bioactive scaffold with osteoconductive and osteoinductive properties [3,17–21].

Biodegradable and bioresorbable polymers such as polylactide (PLA), polyglycolide (PGA), poly(lactide-co-glycolide) (PLGA), poly(epsilon-caprolactone) (PCL) are approved by the World Health Organization and Food and Drug Administration and are very often used as materials in medicine and pharmacy as polymeric prodrugs, for drug delivery or therapeutic systems [22,23]. They have numerous advantages, such as excellent processing characteristics, degradation rates that can be tailored for the intended application, as well as exhibiting unique pharmacokinetics and pharmacological efficacy [23]. PLGA micro and nanoparticles are used for the controlled delivery of several classes of medicaments such as anticancer agents, growth factors, antibiotics, antimicrobial agents, etc. [24]. Metal and metalloid nanoparticles are used in various biomedical applications. For example, silver, gold and platinum are some of the alternative inorganic materials with antimicrobial properties [25]. Selenium nanoparticles have also been reported to possess antibacterial as well as antiviral activities [26]. Additionally, several findings suggest that selenium plays critical roles in a variety of physiological processes and selenium intake may be necessary for bone health [26]. In a recent review, Zeng et al. have summarized current knowledge of the effects of selenium on bone and the underlying mechanisms [27]. Selenium deficiency can retard growth and alter bone metabolism [27–29]. Insufficient selenium intakes have been associated with increased risk to bone disease [29].

The main idea of this work was to design and evaluate a new bioactive material for bone tissue engineering applications, combining bioactive glass (BG) scaffolds and selenium nanoparticles (SeNp), or poly(lactide-co-glycolide) particles with immobilized selenium nanoparticles (PLGA/SeNp) applied as coatings on the BG scaffolds. 3D BG scaffolds were fabricated by the foam replica technique [15]. The samples were characterized by X-ray diffraction (XRD), Fourier transform infrared spectroscopy (FTIR), scanning electron microscopy (SEM), energy dispersive X-ray spectroscopy (EDS) and transmission electron microscopy (TEM). The antibacterial activity of the samples was determined against Gram positive bacteria: *Staphylococcus aureus* (ATCC 25923), *Staphylococcus epidermidis* (ATCC 1228), *Bacillus subtilis* (ATCC 6633), and Gram negative: *Klebsiella pneumoniae* (ATCC 13883).

The present scaffold development corresponds to a growing family of bioactive glass-based scaffolds incorporating antibacterial, functional coatings [12,30–34] although combination of SeNp and BG has not been investigated previously.

2. Materials and methods

2.1. Materials

For the scaffold fabrication, 45S5Bioglass® powder with a composition: 45 SiO_2, 24.5 CaO, 24.5 Na_2O, 6 P_2O_5 in wt%, was used. Fully hydrolyzed PVA (Mw approx. 30,000) (Merck, Darmstadt, Germany) was used to prepare the Bioglass® slurries to make scaffolds. Polyurethane (PU) foam (Eurofoam Deutschland GmbH) with 60 ppi (pores per inch) was used as a template to fabricate scaffolds by the foam replica method described elsewhere [15].

Poly(D,L-lactide-co-glycolide) (PLGA) was obtained from Durect, Lactel, Adsorbable Polymers International and had lactide to glycolide ratio of 50:50. Molecular weight of polymer was 40,000–50,000 g/mol. Polyvinyl pyrrolidone (povidone, PVP) was obtained from Merck Chemicals Ltd. (k-25, Merck, Germany). For the preparing SeNp, sodium selenite (Na_2SeO_3) as well as bovine serum albumin (BSA) were obtained from Sigma–Aldrich, St. Louis, MO. Ascorbic acid was purchased from Microvit, Adisseo, USA ($C_6H_8O_6$, 176.13 g/mol). All other chemicals and solvents were of reagent grade.

2.2. Methods

2.2.1. Synthesis of bioactive glass scaffolds

BG scaffolds were prepared by the foam replica method according to the process introduced earlier [15]. Briefly, glass powder was dispersed in the solution of polyvinyl alcohol (PVA) in deionized water and under constant stirring. In such obtained slurry, PU foams were immersed so that the foam struts were coated with glass particles. PU foam was used as template in this replication method and it was cut into $20 \times 10 \times 10\,mm^3$ samples. After drying at room temperature, the as-coated foams were slowly burned out in order to minimize damage to the glass coating and then the glass network (scaffold) was sintered by heat treatment at 1100 °C [15].

2.2.2. Synthesis of selenium nanoparticles (SeNp)

In the synthesis of SeNp, firstly 217 mg of ascorbic acid have been dissolved in 10 mL distilled water and afterward 12.5 mL of 0.02 M sodium selenite was added into the solvent mixture. The formation of selenium nanoparticles was immediately visualized by a color change of the reactant solution from the colorless to orange. Simultaneously with the addition of sodium selenite, 5 mL of BSA was dropwise added into the solution to stabilize particles i.e. to form BSA-capped SeNp.

2.2.3. Synthesis of PLGA particles with immobilized selenium nanoparticles (PLGA/SeNp)

PLGA/SeNp microspheres were produced using a physicochemical solvent/nonsolvent method. First of all, SeNp were prepared as described above. Afterward, PLGA commercial granules (220 mg) were dissolved in 20 mL acetone over approximately 2 h at room temperature. Then, the solution containing SeNp (0.5 mL) was added to a solution of PLGA in acetone, continuously being homogenized at 21,000 rpm during 15 min, with the resulting solution becoming slightly orange. PLGA/SeNp precipitated by the addition of ethanol (60 mL) and the solution became whitish. Thus obtained solution was very slowly poured into 40 mL of aqueous PVP solution (0.5% w/w) while continuously stirring at 500 rpm by a stirrer. Using PVP as the stabilizer, negative charged PLGA/SeNp particles are produced, i.e. with specific zeta potential, which prevents their agglomeration. Zeta potential of the PLGA/SeNp was measured by Zetasizer Nano ZS particle analyzer (Model ZEN3600, Malvern Instruments, Malvern, UK) and it was determined to be -30.1 ± 0.5 mV.

2.2.4. Coating of 45S5Bioglass® scaffolds by SeNp or by PLGA/SeNp

Sintered 45S5Bioglass® scaffolds were coated with SeNp or with PLGA/SeNp (Fig. 1). The coating was performed by simple soaking/immersing the scaffolds into solution containing SeNp or into solution containing PLGA/SeNp microspheres. This was done with the help of a copper wire gently entwined in the pores of the scaffold. The scaffolds were immersed during the 5 min while continuously stirring at 100 rpm. The coated scaffolds were

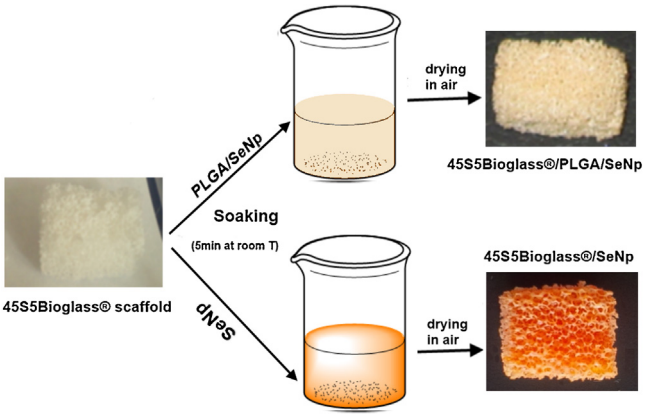

Fig. 1. Schematic diagram showing the steps involved in the coating of 45S5Bioglass® by SeNp or by PLGA/SeNp.

left to dry at room temperature and ambient pressure. Weight percentage of coating on BG scaffolds was determined by thermogravimetric analysis from room temperature to 1000 °C (SETSYS Evo TG-DTA/DSC, Seteram Instrumentation, Lyon, France), with heating rate of 10 °C/min. Precise data was obtained by recording TG curves of uncoated BG scaffolds, SeNp, PLGA and PLGA/SeNp, as well as BG scaffolds coated with SeNp and PLGA/SeNp. Coating of SeNp on BG scaffolds was estimated to be 2.5 wt%, while coating of PLGA/SeNp on BG scaffold was 1.18 wt%. Loading of SeNp in PLGA was 0.15 wt%.

2.3. Characterization

2.3.1. X-ray diffraction

For X-ray diffraction analysis, the samples were firstly grinded and powdered. For identification of the phase composition (phase analysis) of the uncoated scaffolds or scaffolds coated by SeNp or by PLGA/SeNp, X-ray diffraction was used, with a Philips PW 1050 diffractometer with Cu-K$\alpha_{1,2}$ radiation (Ni filter). The measurements were carried out in the 2θ range of 10°–70°, with a scanning step width of 0.05°, and 2 s per step.

2.3.2. Fourier-transform infrared spectroscopy (FTIR)

The quality analysis of the 45S5Bioglass® scaffolds coated by SeNp or by PLGA/SeNp was further performed with FTIR spectroscopy. FTIR spectra of the samples were recorded in the range of 400–4000 cm^{-1} using a Nicolet™ iS™50 FT-IR Spectrometer. FTIR measurements of the samples were carried out to identify the possible interactions between the surface of the BG scaffolds and SeNp or interactions between BG and PLGA/SeNp.

2.3.3. Scanning electron microscopy (SEM)

To analyze the microstructures of the 45S5Bioglass® scaffolds coated by SeNp or by PLGA/SeNp, scanning electron microscopy (SEM) was carried out, on a JEOL-JSM-6610LV instrument. The samples for SEM analysis were coated with gold using the physical vapour deposition (PVD) process. Samples were covered with gold (Leica SCD005 sputter coater), using 30 mA current from the distance of 50 mm during 180 s. The gold coating was used to prevent their charging.

2.3.4. Energy dispersive spectroscopy (EDS)

Energy dispersive spectroscopy (EDS) (model: X-Max Large Area Analytical Silicon Drift connected with INCA Energy 350 Microanalysis System) was used for the elemental characterization of 45S5Bioglass®/SeNp and 45S5Bioglass®/PLGA/SeNp scaffolds.

2.3.5. Transmission electron microscopy (TEM)

Transmission electron microscopy using a JEOL JEM-1400plus instrument provided further morphological characterization of the SeNp incorporated within the PLGA particle, based on the exploration of the individual microstructures.

2.3.6. Antibacterial activity

The antibacterial activities of the tested compounds were investigated against Gram positive bacteria: *S. aureus* (ATCC 25923), *S. epidermidis* (ATCC 1228), *B. subtilis* (ATCC 6633), and Gram

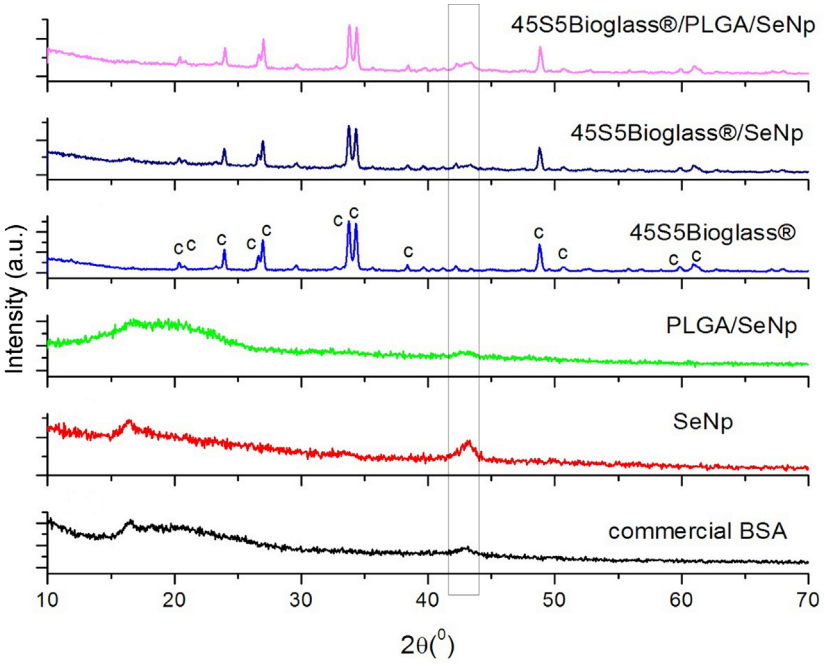

Fig. 2. X-ray diffraction patterns of commercial BSA used in the synthesis for capping SeNp, as-prepared SeNp, PLGA/SeNp, uncoated 45S5Bioglass®, 45S5Bioglass®/SeNp and 45S5Bioglass®/PLGA/SeNp. The c stands for combeite.

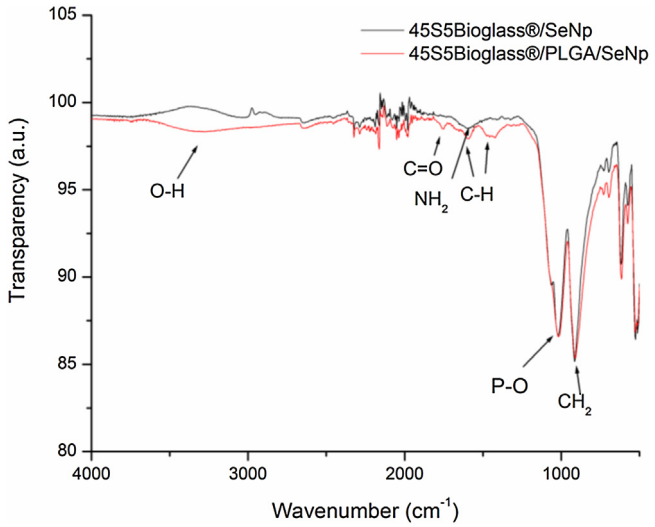

Fig. 3. FTIR spectra of 45S5Bioglass®/SeNp and 45S5Bioglass®/PLGA/SeNp scaffolds.

negative: *K. pneumoniae* (ATCC 13883). A broth microdilution method was used to determine minimum inhibitory concentrations (MICs) of samples. MIC represents the lowest concentration of a compound at which the microorganism does not demonstrate visible growth. MICs were determined according to Clinical and Laboratory Standards Institute (CLSI 2005) [35]. Tests were performed in Müller Hinton broth. Overnight broth cultures were prepared for each strain, and the final concentration in each well was adjusted to 2×10^6 CFU/ml. Uncoated 45S5Bioglass® scaffolds as well as 45S5Bioglass® scaffolds coated by SeNp or by PLGA/SeNp were crushed into powder and then a serial doubling dilutions in 1% dimethylsulfoxide were prepared. A serial doubling dilution of the compounds were prepared in Müller–Hinton broth, in a 96-well microtiter plate, over the range of 1000–12.5 μg/ml. In the tests, 0.05% triphenyl tetrazolium chloride (TTC, Aldrich Chemical Company Inc., USA) was also added to the culture medium as a growth indicator. As a positive control of growth, wells containing only the microorganisms in the broth were used. Bacteria growth was determined after 24 h of incubation at 37 °C. All of the MIC determinations were performed in duplicate, and two positive growth controls were included.

3. Results and discussion

X-ray diffractograms of samples (commercial BSA used in the synthesis for capping SeNp (given here just for comparison purposes), SeNp, PLGA/SeNp, uncoated 45S5Bioglass® scaffolds, 45S5Bioglass® scaffolds coated by SeNp and 45S5Bioglass® scaffolds coated by PLGA/SeNp) are shown in Fig. 2.

P_2O_5, Na_2O, CaO and SiO_2 are the main components of 45S5Bioglass®. The ratio between them is very important considering bioactive character of the material. 45S5Bioglass® is glass where 45 is the weight percentage of SiO_2 and 5 is the molar ratio of Ca to P. Depending on the thermal treatment, bioactive glass powders exhibit different degrees of crystallinity [15,36]. The narrow peaks with high intensity indicate high degree of crystallinity of 45S5Bioglass® scaffold (Fig. 2). PLGA, as well as SeNp, did not exhibit any crystalline peaks because of their amorphous nature (Fig. 2). The only difference between X-ray diffraction patterns of uncoated 45S5Bioglass®, 45S5Bioglass®/SeNp, and 45S5Bioglass®/PLGA/SeNp scaffolds is in peak which belongs to BSA which is used in the synthesis of SeNp as a capping agent. X-ray diffraction patterns of uncoated 45S5Bioglass® as well as 45S5Bioglass®/SeNp scaffolds, and 45S5Bioglass®/PLGA/SeNp scaffolds showed only two phases, both belonging to the family of combeites (c) (Fig. 2) [37]. These phases are low-($Na_{4.2}Ca_{2.8}(Si_6O_{18})$) and high-combeite ($Na_{15.78}Ca_3(Si_6O_{12})$)

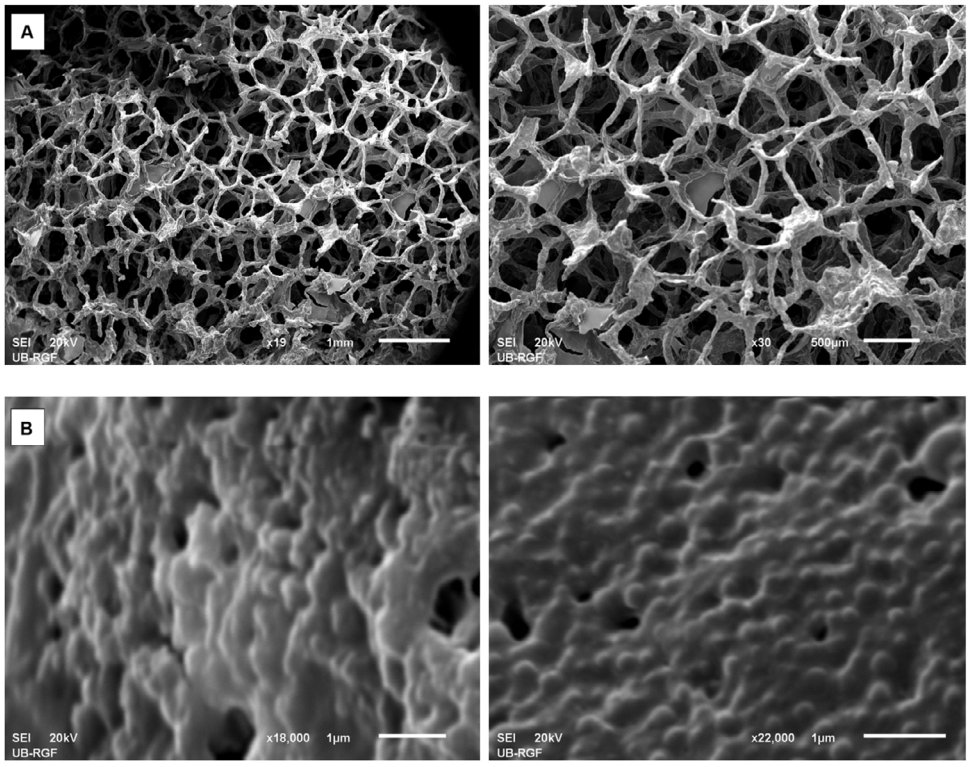

Fig. 4. SEM images showing typical (A) pore (bars 1 mm and 500 μm) and (B) strut microstructures (bars 1 μm) of a 45S5Bioglass® scaffold coated by SeNp. These are representative images of the scaffold cross-sections.

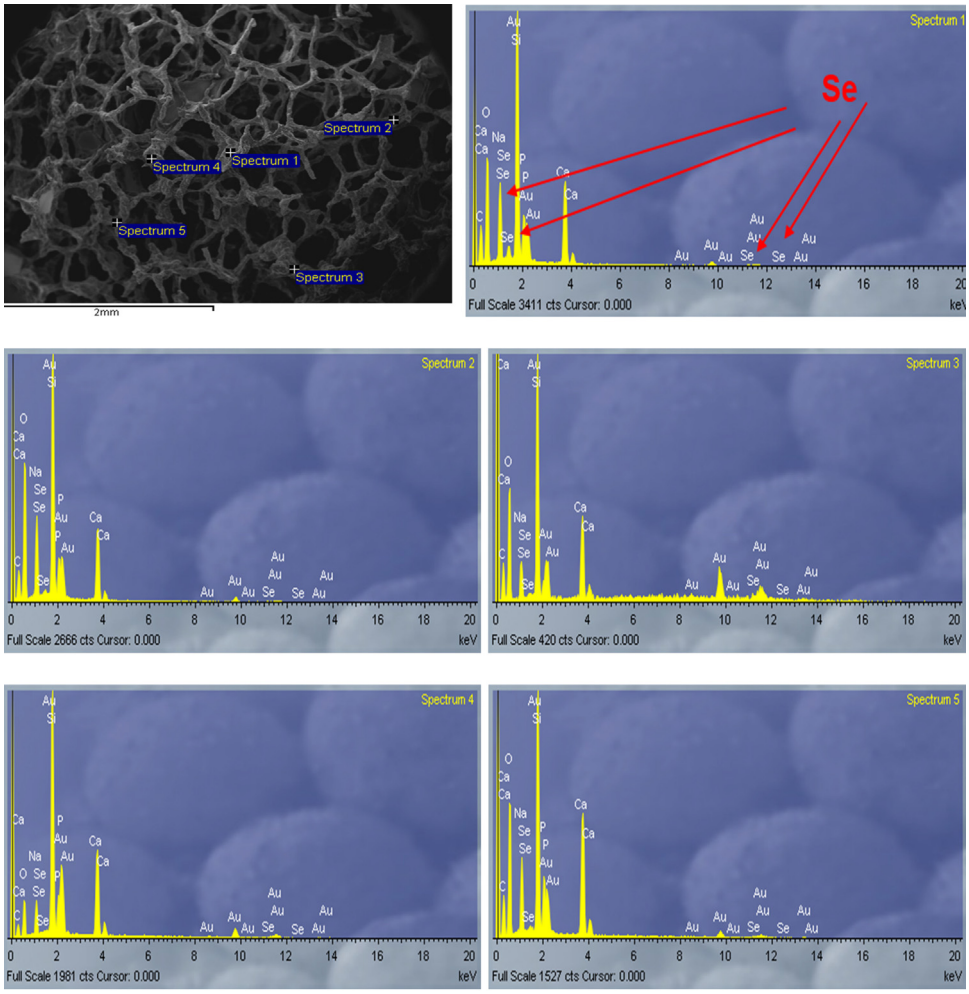

Fig. 5. SEM image showing the surface of SeNp-coated 45S5Bioglass® scaffold, with EDS results on a selected areas of the sample.

[37]. From the literature is known that 45S5Bioglass® has a higher index of bioactivity than hydroxyapatite [38] and bioactivity has been shown to be reduced but not suppressed by crystallization of the phase $Na_2Ca_2Si_3O_9$, as found by Clupper and Hench, which showed amorphous calcium phosphate formation on its surface when it was contacted with simulated body fluid (SBF) [39]. The other crystalline phases, namely $Na_4Ca_4Si_6O_{18}$ also exhibits bioactivity because of its similarity to the phase $Na_2Ca_2Si_3O_9$ [36,37]. $Na_4Ca_4Si_6O_{18}$ and $Na_{15}Ca_{3.84}Si_{12}O_{36}$ phases can be considered as forerunner phases for low- ($Na_{4.2}Ca_{2.8}(Si_6O_{18})$) and high-combeite ($Na_{15.78}Ca_3(Si_6O_{12})$), respectively [37] meaning that 45S5Bioglass®/SeNp, and 45S5Bioglass®/PLGA/SeNp scaffolds are also bioactive.

The FTIR spectra of the 45S5Bioglass®/SeNp and 45S5Bioglass®/PLGA/SeNp samples are shown in Fig. 3. FTIR spectroscopy of these samples was performed to ascertain the presence of SeNp or PLGA/SeNp on the scaffolds. As observed, both spectra reveal bands at 3292 cm^{-1}, 2654 cm^{-1}, 1056 cm^{-1}, 1036 cm^{-1}, 940 cm^{-1}, 701 cm^{-1}, 616 cm^{-1} and 524 cm^{-1}. The broad band at 3292 cm^{-1} is attributed to OH^- absorption. The band at 1036 cm^{-1} is associated with P—O vibrational mode [40,41] while the band at 940 cm^{-1} is attributed to CH_2 out-of-plane wag [42]. In the spectra of 45S5Bioglass®/PLGA/SeNp the band at 1744 cm^{-1} is associated with C=O group and 1581 cm^{-1} and 1456 cm^{-1} are associated with C—H group (in CH_3 and —CH_2) [42]. In the spectra of 45S5Bioglass®/SeNp the band at 1580 cm^{-1} corresponds to the NH_2 deformation (amide II band) [42]. Apart from those peaks, no other peaks can be identified.

The microstructures of the prepared 45S5Bioglass®/SeNp scaffolds were examined by SEM (Fig. 4). The images were taken from the interior section of the scaffolds. A highly porous structure and tailored pore shape for specific application, i.e. bone defects, are essential requirements for ideal bone scaffolds. From these SEM images it can be seen that 45S5Bioglass®/SeNp scaffolds have a well interconnected porous structure. The pore size of the scaffold is around 500 μm (Fig. 4). At higher magnification on the strut microstructures of a 45S5Bioglass®/SeNp scaffold, it is visible that the strut is coated by SeNp. SeNp particles on the strut are spherical, fairly uniform and agglomerated.

Fig. 5 shows a SEM micrograph of a SeNp-coated 45S5Bioglass® scaffold, with EDS results on a selected area of the sample. A surface elemental composition analysis of the SeNp-coated 45S5Bioglass® scaffold showed a strong selenium atom signal, along with silicon, calcium, sodium, oxygen, phosphorus and carbon. In the spectra, there are also peaks which belong to gold and this is due to the preparation of the samples for SEM and EDS measurements, i.e. the samples were coated with gold using the physical vapour deposition process. No obvious peaks for other elements or impurities were observed in the spectra. These results further confirm the successful coating of 45S5Bioglass® scaffold with SeNp.

Representative SEM images of 45S5Bioglass®/PLGA/SeNp scaffolds are given in Fig. 6. These SEM images show typical pore

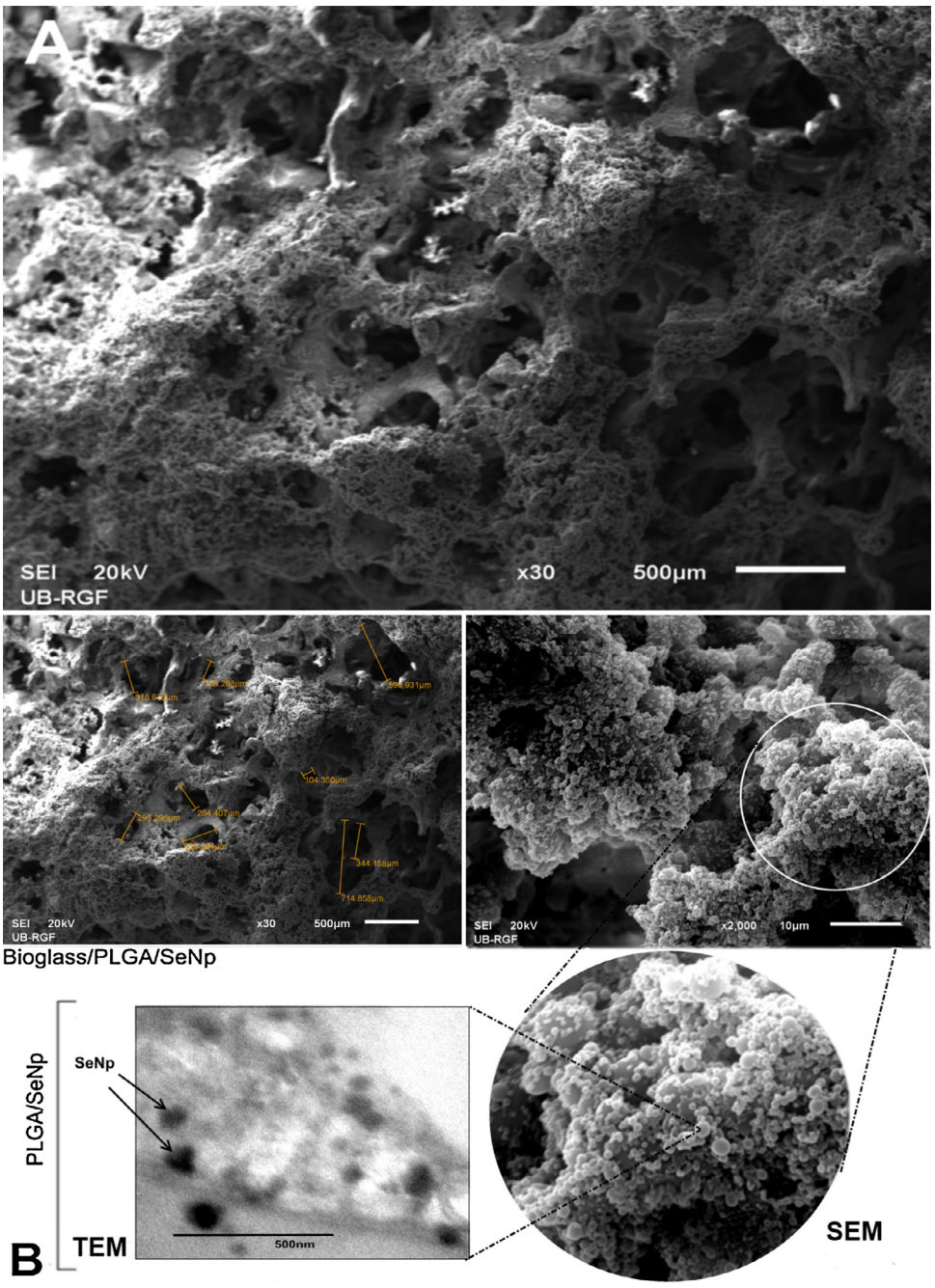

Fig. 6. Representative SEM images (A) of 45S5Bioglass®/PLGA/SeNp scaffolds showing typical pore (bars 500 μm) and strut (bars 10 μm) microstructures of a 45S5Bioglass® scaffold coated by PLGA/SeNp. TEM image (B) of PLGA/SeNp particle from 45S5Bioglass® strut showing heterogeneously distributed SeNps within the PLGA polymer matrix (bars 500 nm).

and struts microstructures of a 45S5Bioglass® scaffold coated by PLGA/SeNp. From these images, it can be seen that in the case of 45S5Bioglass®/PLGA/SeNp scaffolds pores are less uniform compared to 45S5Bioglass®/SeNp scaffolds. PLGA/SeNp particles are spherical in shape and with sizes around 1 μm or less. It is apparent that in both cases the coatings reduce the porosity of scaffolds however given the large size of pores in the as-fabricated scaffolds, the coated samples still exhibit a suitable pore structure (not quantified in this study). Fig. 6 shows also a TEM image of PLGA/SeNp particle from a 45S5Bioglass® scaffold strut showing heterogeneously distributed SeNp within the PLGA polymer matrix. SeNp particles are spherical-shaped.

Energy dispersive spectroscopy was also used for the surface elemental composition analysis of the 45S5Bioglass® scaffold coated with PLGA/SeNp. The EDS spectra showed that the main elements of the 45S5Bioglass®/PLGA/SeNp scaffolds are carbon, oxygen, calcium, sodium and silicon (Fig. 7). Peaks which belong to selenium are also present in the spectra. Peaks of gold were from the sputter coated layer. No peaks for other elements or impurities were observed in the spectra. The EDS analysis of the PLGA/SeNp coated 45S5Bioglass® scaffold showed a much more intense presence of carbon and oxygen compared to 45S5Bioglass®/SeNp scaffold (Fig. 5) thus indicating the coating of scaffold by PLGA/SeNp.

The antimicrobial activity of the samples SeNp, 45S5Bioglass®/SeNp, 45S5Bioglass®/PLGA/SeNp and uncoated 45S5Bioglass® scaffolds was examined. Minimal inhibitory concentrations of samples were determined using a broth microdilution

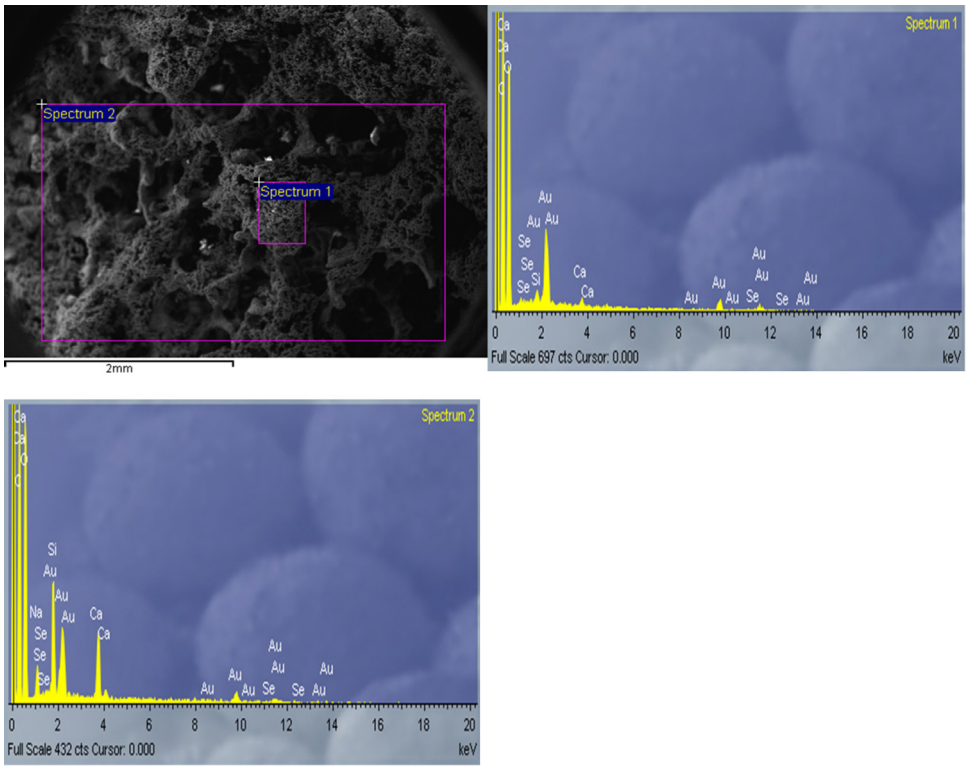

Fig. 7. SEM image showing the surface of 45S5Bioglass®/PLGA/SeNp scaffold, with EDS results on selected areas of the sample.

assay against Gram positive bacteria: *S. aureus* (ATCC 25923), *S. epidermidis* (ATCC 1228), *B. subtilis* (ATCC 6633), and Gram negative: *K. pneumoniae* (ATCC 13883) (Fig. 8).

Hospital-acquired infections (nosocomial infections – not present nor incubating at admission) are caused by bacteria and other pathogens and the most common of these infections are infections associated with orthopedic devices and surgical implants. Infections that are associated with a variety of surgical implants have clinical and economic consequences and often result in serious disabilities [43]. *Staphylococcus* is a group of bacteria and, while *S. epidermidis* is not usually pathogenic, *S. aureus* is considered to be the most dangerous in this group. It can cause a number of diseases and infections range from mild to life threatening. However, even *S. epidermidis*, such as *B. subtilis*, could cause serious infections in patients with compromised immune systems. The Gram-negative bacteria, *K. pneumoniae* also may colonize sites when the host defenses are compromised and cause a variety of lung, bone, heart and bloodstream infections [44]. All of them may be highly resistant to traditional antibiotic therapies [25,45].

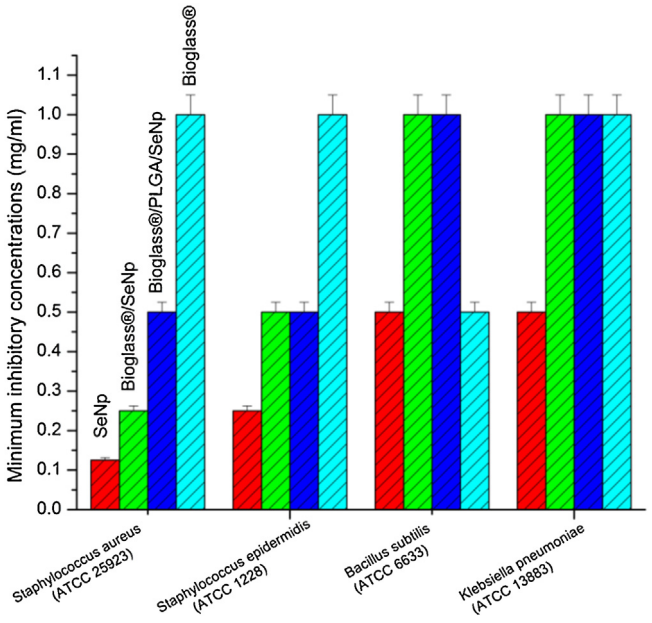

Fig. 8. Antibacterial activity of SeNp, 45S5Bioglass®/SeNp, 45S5Bioglass®/PLGA/SeNp and uncoated 45S5Bioglass®. Minimal inhibitory concentrations of samples were determined using a broth microdilution assay against Gram positive bacteria: *Staphylococcus aureus* (ATCC 25923), *Staphylococcus epidermidis* (ATCC 1228), *Bacillus subtilis* (ATCC 6633), and Gram negative: *Klebsiella pneumoniae* (ATCC 13883).

From the literature is known that selenium nanoparticles are very important for bone health [27,28] but also could serve as antibacterial agent. The role of SeNp as antibacterial agent has been supported in several recent studies [26,46,47].

Results of this study (Fig. 8) provided the evidence of a considerable antibacterial activity against *S. aureus* (ATCC 25923) and *S. epidermidis* (ATCC 1228), in the presence of SeNp as well as in the presence of samples 45S5Bioglass®/SeNp and 45S5Bioglass®/PLGA/SeNp. SeNps also inhibited growth of *B. subtilis* and *K. pneumoniae*.

In the literature, several mechanisms by which nanoparticles may exhibit antimicrobial activity have been proposed [48,49]. Nanoparticles may express better antimicrobial activity compared to conventional preparations due to their large surface-to-mass ratio, better penetration through the cell membrane to affect the intracellular processes from the inside, surface charge, etc. A better understanding of the antibacterial activity of SeNp would require a proper investigation of the membrane-bound and intracellular nanoparticles.

4. Conclusion

45S5Bioglass®-based scaffolds have been synthesized by the foam replica method and additionally coated by SeNp or by PLGA with immobilized SeNp. The coating of BG scaffolds by spherical, amorphous SeNp or by PLGA/SeNp microspheres was confirmed by XRD, FTIR, SEM and EDS analyses. SeNp, 45S5Bioglass®/SeNp and 45S5Bioglass®/PLGA/SeNp scaffolds showed a considerable antibacterial activity against Gram positive bacteria *S. aureus* and *S. epidermidis*, one of the main causative agents of orthopedic infections. Our data suggest that 45S5Bioglass®/SeNp and 45S5Bioglass®/PLGA/SeNp scaffolds are promising candidates for applications in the bone tissue engineering field since it is expected that such scaffolds coated by SeNp or coated by PLGA with immobilized SeNp will exhibit a combination of desirable properties in one device, i.e. controlled drug-delivery function, promotion of bone regeneration and elimination of possible inflammatory responses or infections. Future studies will consider investigating the cell biology response to these scaffolds and in vivo studies.

Acknowledgements

The authors acknowledge the financial support from the German Academic Exchange Service (DAAD) and the Ministry of Education, Science and Technological Development of the Republic of Serbia through the Serbian-German bilateral project no. 451-03-01858/2013-09/2 (DAAD project-ID 57060741). The Ministry of Education, Science and Technological Development of the Republic of Serbia supported this work financially through the project Grant no. III45004. The authors would like to express gratitude to Jadranka Milikić for the technical assistance during the experiments, Suzana Erić for performing the SEM, Ana Mraković for the FTIR measurements and Ljljana Veselinović for performing the XRD measurements.

References

[1] A.J. Salgado, O.P. Coutinho, R.L. Reis, Macromol. Biosci. 4 (2004) 743.
[2] A.R. Amini, C.T. Laurencin, S.P. Nukavarapu, Crit. Rev. Biomed. Eng. 40 (2012) 363.
[3] K. Rezwan, Q.Z. Chen, J.J. Blaker, A.R. Boccaccini, Biomaterials 27 (2006) 3413.
[4] J.F. Mano, R.A. Sousa, L.F. Boesel, N.M. Neves, R.L. Reis, Compos. Sci. Technol. 64 (2004) 789.
[5] H. Shin, S. Jo, A.G. Mikos, Biomaterials 24 (2003) 4353.
[6] D.Y. Kwon, J.S. Kwon, S.W. Shim, J.H. Park, J. Lee, J.H. Kim, W.D. Kim, M.S. Kim, J. Mater. Chem. B 2 (2014) 1689.
[7] L.L. Hench, I. Thompson, J. R. Soc. Interface 7 (2010) S379.
[8] S. Wu, X. Liu, K.W.K. Yeung, C. Liu, X. Yang, Mater. Sci. Eng. Rep. 80 (2014) 1.
[9] L.L. Hench, J.M. Polak, Science 295 (2002) 1014.
[10] C.T. Laurencin, H.H. Lu, in: J.E. Davies (Ed.), Bone Engineering, Em Squared Incorporated, Toronto, Canada, 2000, pp. 462–472.
[11] R. Zhang, P. Ma, J. Biomed. Mater. Res. 45 (1999) 285.
[12] A. Philippart, A.R. Boccaccini, C. Fleck, D.W. Schubert, J.A. Roether, Expert Rev. Med. Devices 12 (2015) 93.
[13] L.C. Gerhardt, K.L. Widdows, M.M. Erol, A. Nandakumar, I.S. Roqan, T. Ansari, A.R. Boccaccini, J. Biomed. Mater. Res. A 101A (2013) 827.
[14] D. Rohanová, A.R. Boccaccini, D.M. Yunos, D. Horkavcová, I. Březovská, A. Helebrant, Acta Biomater. 7 (2011) 2623.
[15] Q.Z. Chen, I.D. Thompson, A.R. Boccaccini, Biomaterials 27 (2006) 2414.
[16] P. Fabbri, L. Valentini, J. Hum, R. Detsch, A.R. Boccaccini, Mater. Sci. Eng. C: Mater. Biol. Appl. 33 (2013) 3592.
[17] D. Huang, Y. Zuo, Q. Zou, L. Zhang, J. Li, L. Cheng, J. Shen, Y. Li, J. Biomater. Sci. Polym. Ed. 22 (2011) 931.
[18] U. Gbureck, T. Holzel, C.J. Doillon, F.A. Muller, J.E. Barralet, Adv. Mater. 19 (2007) 795.
[19] V. Mouriño, P. Newby, A.R. Boccaccini, Adv. Eng. Mater. 12 (2010) B283.
[20] C. Vitale-Brovarone, M. Miola, C. Balagna, E. Verné, Chem. Eng. J. 137 (2008) 129.
[21] E.P. Brennan, J. Reing, D. Chew, J.M. Myers-Irvin, E.J. Young, S.F. Badylak, Tissue Eng. 12 (2006) 2949.
[22] N. Filipović, M. Stevanović, J. Nunić, S. Cundrič, M. Filipič, D. Uskoković, Colloids Surf. B 117 (2014) 414.
[23] M. Stevanović, I. Bračko, M. Milenković, N. Filipović, J. Nunić, M. Filipič, D.P. Uskoković, Acta Biomater. 10 (2014) 151.
[24] S. Acharya, S.K. Sahoo, Adv. Drug Deliv. Rev. 63 (2011) 170.
[25] M. Stevanović, V. Uskoković, M. Filipović, S.D. Škapin, D. Uskoković, ACS Appl. Mater. Interfaces 5 (2013) 9034.
[26] P.A. Tran, T.J. Webster, Int. J. Nanomed. 6 (2011) 1553.
[27] H. Zeng, J.J. Cao, G.F. Combes Jr., Nutrients 5 (2013) 97.
[28] R. Moreno-Reyes, D. Egrise, J. Neve, J.L. Pasteels, A. Schoutens, J. Bone Miner. Res. 16 (2001) 1556.
[29] J.J. Cao, B.R. Gregoire, H. Zeng, J. Nutr. 142 (2012) 1526.
[30] J. Rivadeneira, A.L. Di Virgilio, M.C. Audisio, A.R. Boccaccini, A.A. Gorustovich, J. Appl. Microbiol. 116 (2014) 1438.
[31] X. Chatzistavrou, J.C. Fenno, D. Faulk, S. Badylak, T. Kasuga, A.R. Boccaccini, P. Papagerakis, Acta Biomater. 10 (2014) 3723.
[32] F. Pishbin, V. Mouriño, J.B. Gilchrist, D.W. McComb, S. Kreppel, V. Salih, M.P. Ryan, A.R. Boccaccini, Acta Biomater. 9 (2013) 7469.
[33] A. Simchi, E. Tamjid, F. Pishbin, A.R. Boccaccini, Nanomed. Nanotech. Biol. Med. 7 (2011) 22.
[34] J. Pratten, S.N. Nazhat, J.J. Blaker, A.R. Boccaccini, J. Biomater. Appl. 19 (2004) 47.
[35] Clinical and Laboratory Standards Institute (CLSI), Performance Standards for Antimicrobial Susceptibility Testing, 15th Informational Supplement, CLSI Document M100-S15, Wayne, PA, USA, 2005.
[36] O. Bretcanu, X. Chatzistavrou, K. Paraskevopoulos, R. Conradt, I. Thompson, A.R. Boccaccini, J. Eur. Ceram. Soc. 29 (2009) 3299.
[37] C. Volzone, F.M. Stábile, N. J. Glass Ceram. 3 (2013) 27350.
[38] L.L. Hench, Bioceramics, J. Am. Ceram. Soc. 81 (1998) 1705.
[39] D.C. Clupper, L.L. Hench, J. Non-Cryst. Solids 318 (2003) 43.
[40] E.R. Essien, L.A. Adams, R.O. Shaibu, I.A. Olasupo, A. Oki, Open J. Regen. Med. 1 (2012) 25915.
[41] B. Olalde, N. Garmendia, V. Sáez-Martínez, N. Argarate, P. Nooeaid, F. Morin, A.R. Boccaccini, Mater. Sci. Eng. C: Mater. Biol. Appl. 33 (2013) 3760.
[42] J.B. Lambert, Introduction to Organic Spectroscopy, MacMillan Publishing Company, New York, 1987.
[43] R.O. Darouiche, N. Engl. J. Med. 350 (2004) (1422).
[44] J. de Sanctis, L. Teixeira, D. van Duin, C. Odio, G. Hall, J.W. Tomford, F. Perez, S.D. Rudin, R.A. Bonomo, W.K. Barsoum, M. Joyce, V. Krebs, S. Schmitt, Int. J. Infect. Dis. 25 (2014) 73.
[45] E. Oldfield, X. Feng, Resistance-resistant antibiotics, Trends Pharmacol. Sci. 35 (2014) 664.
[46] P.A. Tran, T.J. Webster, Nanotechnology 24 (2013) (1551) 01.
[47] A.K. Mittal, S. Kumar, U.C. Banerjee, J. Colloid Interface Sci. 431 (2014) 194.
[48] J.T. Seil, T.J. Webster, Int. J. Nanomed. 7 (2767) (2012).
[49] J.A. Lemire, J.J. Harrison, R.J. Turner, Nat. Rev. Microbiol. 11 (6) (2013) 371.